Available online at www.sciencedirect.com
SCIENCE DIRECT®
Chemical Physics Letters 398 (2004) 32–36
CHEMICAL PHYSICS LETTERS
www.elsevier.com/locate/cplett

Phase controlled synthesis of ZnS nanobelts: zinc blende vs wurtzite

Yong Ding [a], Xu Dong Wang [a], Zhong Lin Wang [a,b,*]

[a] School of Materials Science and Engineering, Georgia Institute of Technology, Atlanta, GA 30332-0245, USA
[b] National Center for Nanoscience and Nanotechnology, Beijing 100080, China

Received 1 August 2004; in final form 9 September 2004
Available online 28 September 2004

Abstract

Bulk crystals of ZnS usually take the zinc blende structure. However, the vapor deposited one-dimensional ZnS nanostructures normally take the metastable wurtzite structure. This Letter investigates the conditions under which the formed phase can be controlled between zinc blende and wurtzite in nanomaterials synthesis. The formation of pure zinc blende structured ZnS nanobelts is related not only to the lower deposition temperature (680–750 °C), but also to the size of the Au catalyst particle (<50 nm). Pure wurtzite structured ZnS nanobelts are synthesized in a relatively high deposition temperature (>750 °C) disregard the size of the Au catalyst particles.

1. Introduction

One-dimensional (1D) nanowires and nanobelts of compound semiconductor are of fundamental importance owing to their potential applications as building blocks in nanoelectronics, optoelectronics, resonators, sensors and actuators [1,2]. ZnS, an important II–VI semiconductor, has attracted considerable attention due to its applications in flat-panel displays, electroluminescent devices, infrared windows, sensors and lasers [3–5]. The most stable bulk form of ZnS at room temperature is the zinc blende structure, which can transfer to wurtzite structure after heating to 1020 °C in ambient pressure [6]. Phase control in the growth of ZnS crystal is important, for instance, the different phases show different lattice vibration properties [7] and nonlinear optical coefficients [8].

Recently, several ZnS nanostructures, including nanowires [9] nanobelts/nanoribbons [10], nanosaws [11] and nanocables [12] have been reported. In contrast to the bulk form, the dominant of the ZnS nanostructures takes the wurtzite phase [10,13]. It may be of fundamental interest to investigate the conditions under which the phase of the as-synthesized ZnS nanostructures can be controlled between wurtzite and zinc blend. In this Letter, through a series of designed experiments, we found that the formation of zinc blende structured ZnS nanobelts is related not only to the lower deposition temperature (in our case, 680–750 °C), but also to the size of the Au catalyst particles (smaller than 50 nm). Pure wurtzite structured ZnS nanobelts can be synthesized in a relatively high deposition temperature (above 750 °C) regardless the size of the Au catalyst particles. This study gives a practical guidance for controlling the phase of ZnS nanostructures.

2. Experiments

ZnS nanobelts were synthesized through a vapor–liquid–solid (VLS) process [14]. High-purity ZnS powders were put in an alumina boat located at the center of the alumina tube. The entire length of the tube fur-

* Corresponding author. Fax: +1 404 894 9140.
E-mail address: zhong.wang@mse.gatech.edu (Z.L. Wang).

0009-2614/$ - see front matter © 2004 Elsevier B.V. All rights reserved.
doi:10.1016/j.cplett.2004.09.031

nace is 75 cm. Silicon substrates covered with Au film were placed in the tube at a distance from 5 to 25 cm from the center of the alumina boat. After evacuation of the tube to $\sim 2 \times 10^{-2}$ Torr, a carrier gas of high-purity argon premixed with 5% hydrogen was kept flowing through the tube. The flow rate and pressure inside the tube were kept, respectively, at 50 sccm and 300 Torr throughout the experiment. The furnace was then heated at a rate of 25 °C/min to 800 °C and held at that temperature for 20 min. The furnace temperature was then further raised to 1000 °C and held at that temperature for 50 min. The local temperature distribution and the position of the substrate have been calibrated and the result is presented in Fig. 1a. After the deposition, the furnace was naturally cooled to room temperature. Au thin films with an average thickness around 5 and 10 nm were deposited onto silicon substrate, which produces gold particles of sizes ~35 and ~100 nm, respectively. The deposited products were characterized by scanning electron microscopy (SEM) and transmission electron microscopy (TEM; Hitachi HF2000 and JEOL 4000EX, respectively, operated at 200 and 400 kV).

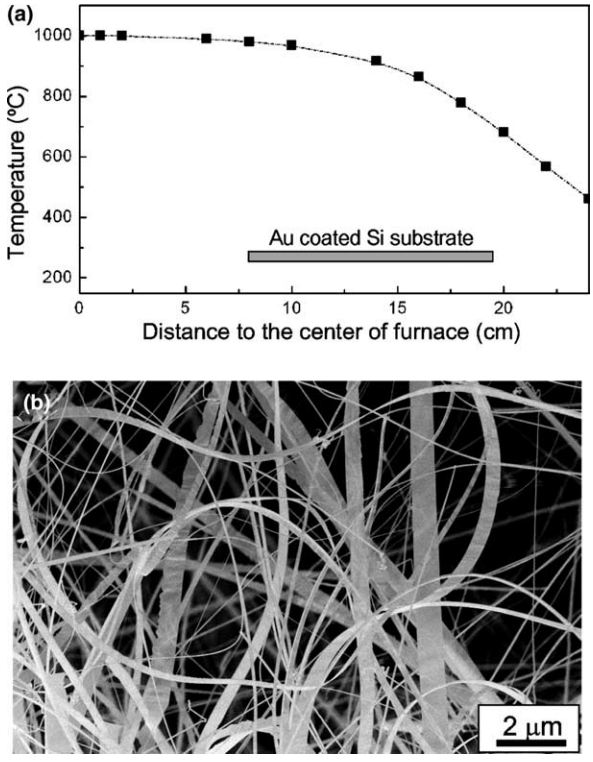

Fig. 1. (a) A plot of the relationship between the local temperature and the distance to the center of the furnace for the experimental set up used in our experiments. The position of the substrate is illustrated. (b) SEM image recorded from a sample collected in the temperature region of ~720 °C grown using an Au thin film ~5 nm in thickness, which correspond to ~35 nm in particle sizes.

3. Results and discussion

3.1. Nanostructures formed at ~720 °C using 35 nm size Au catalyst particles

The SEM image in Fig. 1b displays the morphologies of the ZnS nanostructures grown in the temperature zone ~720 °C grown with Au catalyst with an average deposition thickness of ~5 nm. Uniform nanobelts and asymmetric nanosaws are the two dominant morphologies of the ZnS nanostructures. The sizes of the nanobelts and nanosaws can be seen clearly in the TEM image as shown in Fig. 2a. The width of the uniform nanobelts is usually under 50 nm, while the width of the nanosaws is over 100 nm. The gold catalyst particles are at the tips of the nanobelts, and their sizes are ~35 nm.

We now determine if the narrower nanobelts and the wider nanosaws are of the same crystal structure. This analysis relies on selected-area electron diffraction (SAED) and high-resolution TEM (HRTEM). For the narrower nanobelts, Fig. 2b is the SAED pattern from a fine nanobelt shown at the center of Fig. 2a. The diffraction pattern can only be indexed as the zinc blend structure with the incident electron beam parallel to [0 1 1]. The corresponding HRTEM image recorded from the nanobelt is presented in Fig. 2c, revealing that the nanobelt grows along [1 0 0] and takes $\pm(0\bar{1}1)$ as the side surfaces. The inset atomic structure model in Fig. 2c reveals that the nanobelt growth front is a polar surface

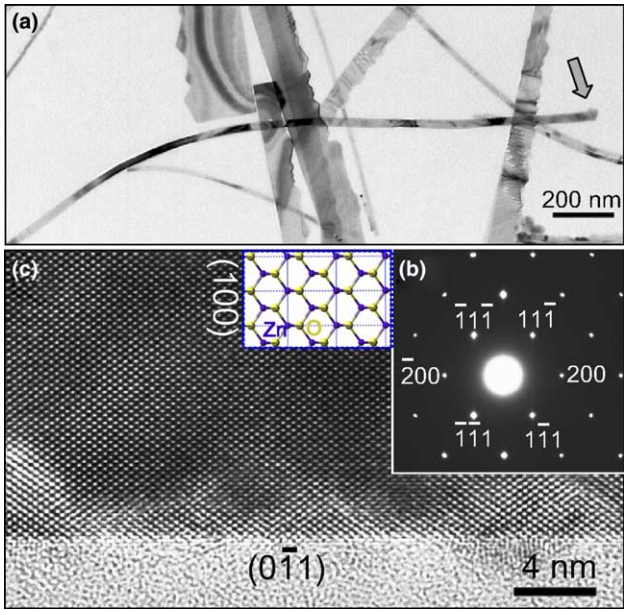

Fig. 2. Structure of narrow nanobelts grown at ~720 °C and using ~35 nm Au particles. (a) TEM image showing the uniform nanobelts and asymmetric nanosaws, (b) SAED pattern and (c) HRTEM image recorded from a narrow nanobelt as pointed in (a), which has the zinc blend structure. The inset in (c) is the atomic model of zinc blende ZnS.

terminated either with Zn or S. From our early study of ZnO [15], the Zn-terminated surface is catalytically more active than the S terminated surface, thus, the growth front could be terminated with Zn, leading to the fastest growth. The HRTEM image shows that the $\pm(0\bar{1}1)$ side surfaces are flat and without reconstruction as viewed along [011]. We have analyzed a number of narrow nanobelts and all of them have the zinc blend structure.

We now examine the nanosaws. Although the nanosaws were deposited in the same temperature zone, but they do not take the same structure as the narrow uniform nanobelt as shown in Fig. 2. The structure details of the nanosaw are displayed in Fig. 3. The SAED pattern shown in Fig. 3b suggests that the zinc blend (as indicated by arrowheads) and wurtzite (rectangle marked diffraction spots) structures co-existence in the nanosaw. The HRTEM images in Fig. 3c–e are recorded from different areas of the nanosaw, as marked in Fig. 3a, to reveal the local structures. The main body of the saw is wurtzite structure as shown in Fig. 3c, but the teeth are zinc blende structure (Fig. 3d). The transformation from wurtzite to zinc blend occurs at root of the saw teeth (Fig. 3e). Comparing the atomic model inserted in Fig. 2c with the image shown in Fig. 3c, the two structures can be easily identified.

For the zinc blend structure, the (111) plane is the close packing plane; the (0001) plane of wurtzite is the close packing plane. The relationship between zinc blend and wurtzite is a change in stacking sequence of the atomic planes. Zinc blend is a stacking of ABCABC parallel to the close packing plane, and wurtzite is a stacking of ABAB.

The formation of the nanosaw morphology can be explained using a combination of vapor–liquid–solid (VLS) and the self-catalyzed growth process in two-steps [15]. First, the Au catalyst guides the fastest growth along $[01\bar{1}0]$ to form the wurtzite structured nanobelt, with $\pm(2\bar{1}\bar{1}0)$ and $\pm(0001)$ as its top/bottom and side surfaces; the sulfur terminated $(000\bar{1})$ side surface is inert and is stable, while the zinc terminate (0001) surface is catalytically active and could initiate growth in the direction perpendicular to the nanobelt. In the second growth process, small islands can nucleate on the flat (0001) surface, and each island epitaxially grows up to form a saw tooth, but strain is produced when the two adjacent teeth meet. This result is proved by the existence of mismatch dislocations in the region between the two teeth (islands), as displayed in Fig. 3e. Each island has the zinc blend structure. If the growth front of the teeth is $(11\bar{1})$ plane, which matches to the zinc terminated (0001) plane, the two side surfaces of the teeth are $(01\bar{1})$ and $(31\bar{1})$ planes as marked in the atomic model in Fig. 3d. The high-index $(31\bar{1})$ plane has higher surface energy, thus, it is preferred to reconstruct into a series $(11\bar{1})$ and (100) facets.

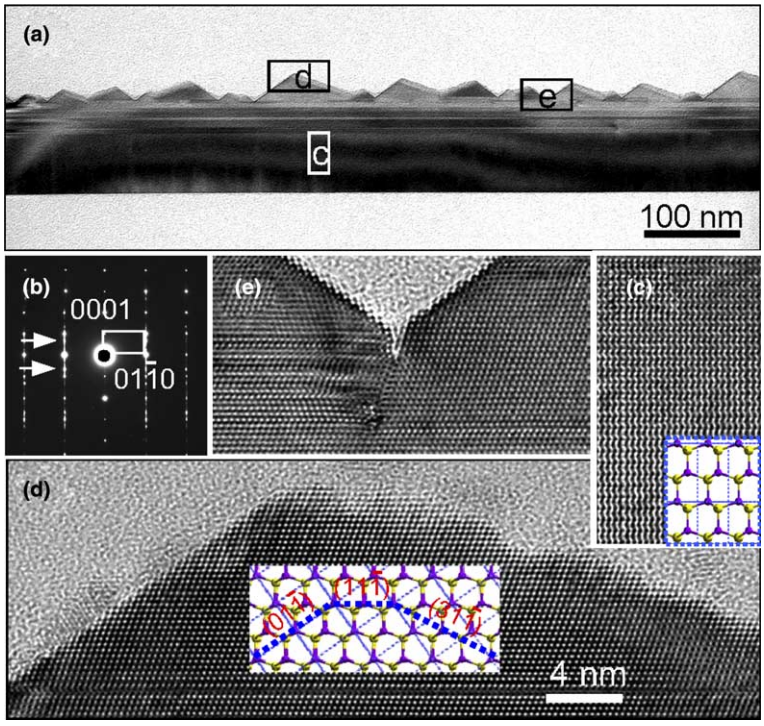

Fig. 3. Structure of nanosaws grown at ~720 °C and using ~35 nm Au particles. (a) Low-magnification TEM image of a nanosaw. (b) SAED pattern of the whole nanosaw, showing the co-existence of the zinc blend and wurtzite phases. (c–e) HRTEM images recorded from the rectangle enclosed areas labeled in (a). The inset in (c) gives the atomic model of wurtzite phased ZnS, and the inset in (d) is for the zinc blend.

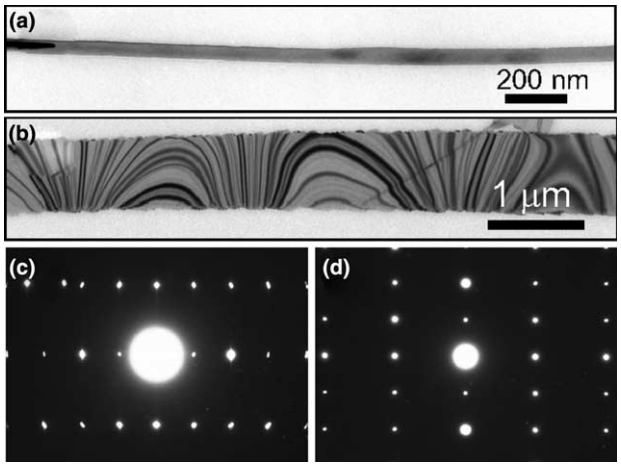

Fig. 4. Structure of nanobelts grown at >750 °C and using ~35 nm Au particles. (a, b) TEM images a narrow and wide nanobelts, and (c, d) are corresponding SAED patterns, respectively.

3.2. Nanostructure formed at temperatures >750 °C using Au catalyst particles of 35 nm in size

We now analyze the nanostructures formed at temperatures higher than 750 °C using the 35 nm size Au catalyst particles. Our results indicate that the higher deposit temperature results in the formation of pure wurtzite nanobelts as shown in Fig. 4. No matter the size of the nanobelts is, the SAED patterns recorded from them indicate that they are all of wurtzite structure (seeing Fig. 4c, d). The fine nanobelts always take [0 0 0 1] as they growth direction and $\pm(2\bar{1}\bar{1}0)$ and $\pm(01\bar{1}0)$ as top/bottom and side surfaces. The nanobelts growing along $[0\,1\,\bar{1}\,0]$ directions are normally with larger width.

3.3. Nanostructure formed using Au catalyst particles of 100 nm in size

In order to find the relationship between the phase formation and the size of the catalyst particles, we designed another experiment using a thicker Au film of an average thickness ~10 nm, which produces Au particles of ~100 nm in sizes. The SEM image from the sample collected in a deposition temperature zone of ~720 °C is shown in Fig. 5a. Similar to those shown in Figs. 2 and 3, uniform nanobelts and asymmetric nanosaws are the two main morphologies (Fig. 5b, c). The Au catalysts have an average size around 100 nm, which guide the growth of larger size ZnS nanostructures. In order to identify the phase of each nanostructures, SAED patterns from many nanostructures have been recorded. The diffraction pattern presented in Fig. 5e is from the nanobelt shown in Fig. 5c, which is a pure wurtzite phase. The pattern in Fig. 5d is recorded from the nanosaw in Fig. 5b, showing that it is a mixture of wurtzite with zinc blend, similar to the nanosaw presented in Fig. 3. After examining over 50 nanobelts, no pure zinc blende phased nanobelts have been found even for the small width nanobelts. This is a distinct difference from the nanostructure grown using ~35 nm size Au catalyst particles.

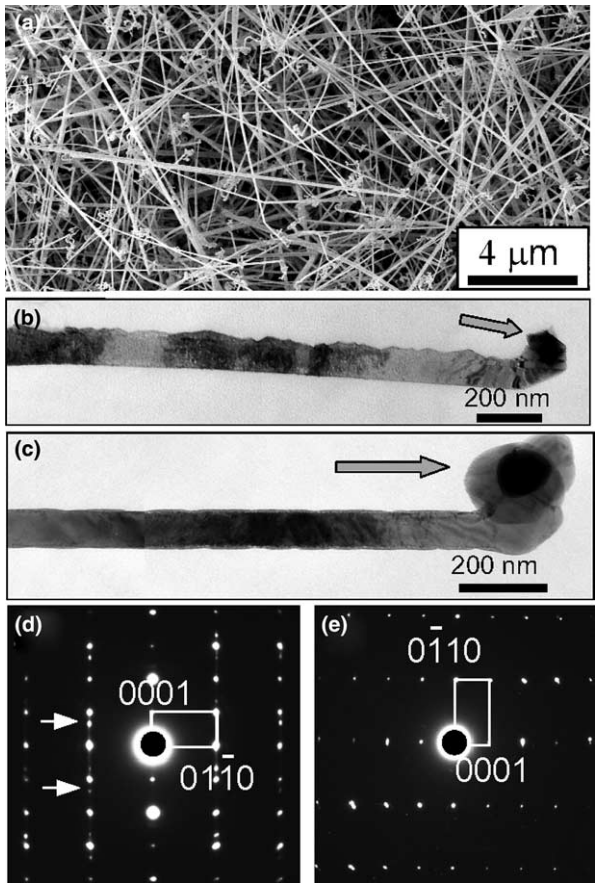

Fig. 5. Structure of nanobelts and nanosaws grown at ~720 °C and using ~100 nm Au particles. (a) SEM image of the sample. (b, c) TEM images of a nanosaw and nanobelt, and (d, e) are corresponding SAED patterns, respectively. The nanosaw is a mixture of zinc blend and wurtzite, and the nanobelt is wurtzite structure.

After analyzing the as-received product, nanostructures formed in temperature zones of higher than 750 °C all have wurtzite structure. If the wurtzite phased ZnS is needed, the high deposit temperature is the key, no matter about the size of the Au catalyst particles.

4. Conclusion

In the VLS deposition process, by adjusting the synthesis conditions, we can control the deposited ZnS nanostructures being zinc blend phase, wurtzite phase or a mixture. The low deposition temperature of 680–750 °C and small Au catalyst particles (<50 nm) produce zinc blend ZnS nanobelts. Pure wurtzite structured ZnS nanobelts are synthesized at a higher deposition temperature (above 750 °C) disregard the size of the Au

catalyst particles. The nanosaws are usually a mixture of zinc blend teeth with a wurtzite body. This study gives guidance for controlling the phase of the as-synthesized ZnS nanostructures.

Acknowledgement

The research was sponsored by NSF and NASA.

References

[1] Z.L. Wang (Ed.), Nanowires and Nanobelts, Metal and Semiconductor, Nanowires, vol. I, Kluwer Academic Publishers, New York, 2003.
[2] Z.L. Wang (Ed.), Nanowires and Nanobelts, Nanowires and Nanobelts of Functional Materials, vol. II, Kluwer Academic Publishers, New York, 2003.
[3] M. Bredol, J. Merichi, J. Mater. Sci. 33 (1998) 471.
[4] P. Calandra, M. Goffredi, V.T. Liveri, Colloids Surf. A 160 (1999) 9.
[5] T.V. Prevenslik, J. Lumin. 87–89 (2000) 1210.
[6] S.B. Qadri, E.F. Skelton, D. Hsu, A.D. Dinsmore, J. Yang, H.F. Gray, B.R. Ratna, Phys. Rev. B 60 (1999) 9191.
[7] O. Brafman, S.S. Mitra, Phys. Rev. 171 (1968) 931.
[8] D.R. Lide (Ed.), Handbook of Chemistry and Physics, CRC Press, Boca Raton, FL, 1981.
[9] Y. Jiang, X.M. Meng, J. Liu, Z.Y. Xie, C.S. Lee, S.T. Lee, Adv. Mater. 15 (2003) 323.
[10] C. Ma, D. Moore, J. Li, Z.L. Wang, Adv. Mater. 15 (2003) 228.
[11] D. Moore, C. Ronning, C. Ma, Z.L. Wang, Chem. Phys. Lett. 385 (2004) 8.
[12] Y.C. Zhu, Y. Bando, Y. Uemura, Chem. Commun. 7 (2003) 836.
[13] Y. Jiang, X.M. Meng, C.S. Lee, S.T. Lee, Adv. Mater. 15 (2003) 1195.
[14] R.S. Wagner, W.C. Ellis, Appl. Phys. Lett. 4 (1964) 89.
[15] Z.L. Wang, X.Y. Kong, J.M. Zuo, Phys. Rev. Lett. 91 (2003) 185502.